We are IntechOpen,
the world's leading publisher of Open Access books
Built by scientists, for scientists

6,900
Open access books available

185,000
International authors and editors

200M
Downloads

Our authors are among the

154
Countries delivered to

TOP 1%
most cited scientists

12.2%
Contributors from top 500 universities

CLARIVATE ANALYTICS
BOOK CITATION INDEX
INDEXED

WEB OF SCIENCE™

Selection of our books indexed in the Book Citation Index
in Web of Science™ Core Collection (BKCI)

Interested in publishing with us?
Contact book.department@intechopen.com

Contact-less Assessment of In-vivo Body Signals Using Microwave Doppler Radar

Shahrzad Jalali Mazlouman, Kouhyar Tavakolian,
Alireza Mahanfar and Bozena Kaminska
Simon Fraser University, School of Engineering Science
8888 University Drive, V5A 1S6
Burnaby, BC, Canada

1. Introduction

Every seven minutes in Canada, someone dies from heart disease or stroke. Cardiovascular disease (heart disease, diseases of the blood vessels and stroke) accounts for the death of more Canadians than any other disease (Heartandstroke, 2004). Early detection and treatment of symptoms and abnormalities can significantly decrease this rate. Therefore, the heart-related signals are the most important vital signals to monitor. For many years, extensive work has been devoted to finding low-cost, convenient, ubiquitous solutions to monitor heart signals in the everyday life. While these devices are beneficial, they have the disadvantage of requiring physical contact with the patient. Examples include chest straps to monitor the electrocardiogram (ECG) signal, gel for ultrasounds (echocardiography), heavy accelerometer sensor for seismocardiogram and electrodes for impedance cardiography (ICG) and oximetery. In addition, most of the existing methods require special expertise to use. The ideal solution would include a non-obtrusive method that can be used continuously and in everyday life without touching the patient and without requiring special expertise.

From another point of view, seniors are becoming the fastest growing segment of the population in North America (Michahelles et al., 2004). This trend creates a new demand for health care. Availability of cost-efficient, wearable, non-invasive, real-time methods of monitoring body signals that can be used at home can save a significant fraction of costs for the health care system while providing efficient care to the elderly. Consequently, there is a growing demand for devices that allow remote monitoring of health related parameters and transferring the recorded data to a physician via telephone, internet, or cellular phone networks, in case of sensing any abnormalities or symptoms.

Such non-invasive methods can also be beneficial for monitoring the effectiveness of treatment procedures for patients in the hospital or at home without requiring physical contact, thereby allowing long-term health care monitoring at almost no compromise in the patient's mobility or ordinary lifestyle. As an example, in this chapter, a new method for monitoring of congestive heart failure patients using the radar technology is proposed. In addition, in-vivo body signals monitoring, in particular heart and breathing rate monitoring,

can provide safety in critical situations such as car driving, by initiating actions such as automatic control, stop and urgent call upon reading of an emergency call by the developed sensor (Michahelles et al., 2004).

In this chapter, the basics of Microwave Doppler radar systems are investigated as a cost-efficient, non-invasive, and ubiquitous solution for continuous monitoring of in-vivo body signals; in particular, non-invasive sensing of cardiac, respiratory, and arterial movements. Microwave Doppler radar can detect motions and velocity based on Doppler effect; therefore, a variety of body signals including the mechanical motions of the chest because of heart beat (the radar seismocardiogram, R-SCG) as well as the blood flow velocity in major blood vessels can be monitored. Parameters such as heart-rate, hemodynamic parameters, blood flow velocity and respiration rate can be measured using these devices. Microwave Doppler radar systems do not require direct contact with the body and can function through blankets or clothing.

Although laboratory demonstrations of the use of Doppler radar for cardiovascular and respiratory measurements date back to the late 1970's and early 1980's (Lin, 1975; Lin, 1979), cost-efficient, wearable body signal monitoring devices have not been reported until very recently; when implementation of low-cost, low-power, battery-operated devices is more feasible than ever by virtue of the availability and advances in high-integration technologies, signal processing techniques, and high-speed communication networks.

Depending on the application, Microwave Doppler radar systems may use a continuous-wave or a time-gated radar signal. Continuous-wave Doppler radar have been shown to be comparable and even exceeding the conventional impedance cardiography methods for measuring the mechanical activity of the heart, as well as for measuring the heart-rate variability (HRV) (Staderini, 2002a). In fact, the derivative of the radar signal shows better correlations with the impedance cardiogram signal (ICG) (Thijs et al., 2005). Some signals have been confirmed to be more clear on the captured radar signal than on the ICG, for example, the opening of the atrium and the mitral valve (Thijs et al., 2005).

A continuous Microwave Doppler radar based system was developed in the centre for integrative bio-engineering research (CiBER lab) of Simon Fraser University (Tavakolian et al, 2008a). The developed device is completely implemented on board and is the first reported device that can be used independently as a stand-alone system or can be connected to a PC. This device was tested to measure the heart and respiration rate of human subjects and demonstrated a noticeable accuracy of 91.35% for respiration rate, and 92.9% for heart rate. More importantly, this system was used to extract R-SCG signal as is discussed in the next sections.

The structure of this book chapter is as follows. In Section 2, body signals that can potentially be measured using the Doppler radar system are introduced. Special emphasize has been given to a class of infrasonic cardiac signals, that radar extracted R-SCG signal belongs to it. In this section technical background such as the Doppler Effect, the radar system, and the ultra-wideband radar are discussed. In Section 3, details of the Microwave Doppler radar systems are discussed and analyzed and the related equations are derived. The building blocks are introduced and design specifications and requirements are calculated. Section 4 is devoted to practical implementation of the Microwave Doppler radar based system that was designed and implemented in the CiBER lab.

2. Background

2.1 Infrasonic Cardiac Signals

Radar seismocardiogram (R-SCG) belongs to a category of cardiac signals that have their main components in the infrasonic range (less than 20 Hz) and reflect the mechanical function of the heart as a pump. During the past century, extensive research has been conducted on interpretation of these signals in terms of their relationship to cardiovascular dynamics and their possible application in cardiac abnormality diagnostics. Signals such as ballistocardiogram (BCG), seismocardiogram (SCG), apexcardiogram (ACG) and radar seismocardiogram reflect the displacement, velocity, or acceleration of the body in response to the heart beating.

Different methods that were used to acquire these signals are shown in Fig. 1. R-SCG is recorded by contactless radar method, SCG and ACG are recorded by attaching sensors to the chest and BCG is recorded by measuring the changes of the center of mass of the whole body. The ACG acquisition is very similar to SCG, except for the recording site on the chest, which is the point of maximum impulse for ACG and the sternum for most SCG definitions, as is explained in the next section. A contactless method of recording ACG has also been proposed using microwave radar (Lin, 1979).

The recorded signal morphology will vary with the method employed, but all the techniques appear to signal basically the same events in the cardiac cycle. The basic physiology behind all these signals are as follows: with each heart beat, blood rushes upward and strikes the aortic arch. The impact is great enough to give the whole body an upthrust. When the descending blood slows down, there is a rebound effect which gives the body a downthrust, not as intense as the earlier upthrust.

These signals are normally recorded together with ECG thus, an understanding of the electromechanical performance of the heart can be achieved. In order to better understand the genesis of waves in R-SCG signal, for the first time in this writing, we study these signals in the same context and briefly investigate their similarities and differences.
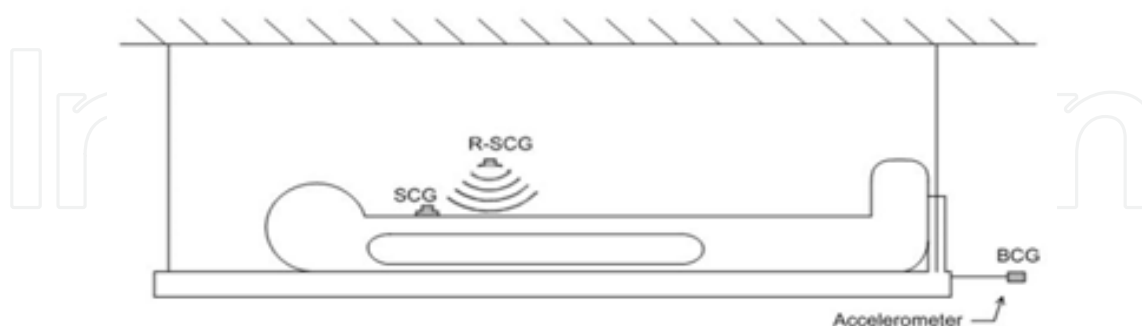

Fig. 1. Different recording schemes for acquistion of infrasonic cardiac signals

2.1.1 Ballistocardiogram (BCG)

The ballistocardiogram is caused by the change of the center of mass of body because of the blood circulation and can be recorded by noninvasive means. In the early 1930s Isaac Starr recognized that the BCG signals closely reflect the strength of myocardial contraction and

function of the heart as a pump. As a result of his valuable research, clinicians and medical experts for almost three decades studied the effects of different heart malfunctions using BCG and proved that these malfunctions can be related to typical patterns on the BCG signal morphology (Starr & Noordergraaf, 1967).

Most types of BCG involve a platform upon which a subject lies supinely. BCG systems were categorized by their natural frequency with respect to the heart's own natural frequency of about 1 Hz. Those BCG apparatuses with higher natural frequencies of 10 Hz to 15 Hz are high frequency BCG (HF-BCG). Those with natural frequencies of approximately 1 Hz are low frequency (LF-BCG) and those lower than 1 Hz are ultra-low frequency (ULF-BCG). Binding and dampening of the BCG apparatus can be thought of as filtering its resultant signal such that frequencies below its natural frequency are removed. Thus, HF-BCG removes more of the low frequency spectrum, and so it reflects forces, whereas ULF-BCG measures displacement better. The physical basis of these BCG apparatuses is examined in elegant detail by Noordergraaf (Starr & Noordergraaf, 1967).

The ideal BCG waveform consists of seven waveforms peaks labeled G through N as defined by the American Heart Association. H is the first upward deflection after electrocardiograph (ECG) R-wave on the acceleration BCG when recorded simultaneously. The letter I is the downward wave immediately after H, and lastly the letter J is the upward wave after I. The L, M and N waves correspond to the diastolic phase of the cardiac cycle, all the waves can be seen in Fig. 2. (Scarborough & Talbot 1956).

In addition to a number of clinical studies that have been performed with BCG, specialized BCG instruments, including beds (Jensen et al., 1991), chairs (Junnila et al., 2008) and weight scale (Inan et al., 2008), have been developed by different research groups. However, due to the unrefined nature of the previous BCG signal acquisition technologies, the lack of interpretation algorithms, and the lack of practical devices, the current health care systems do not use BCG for clinical purposes.
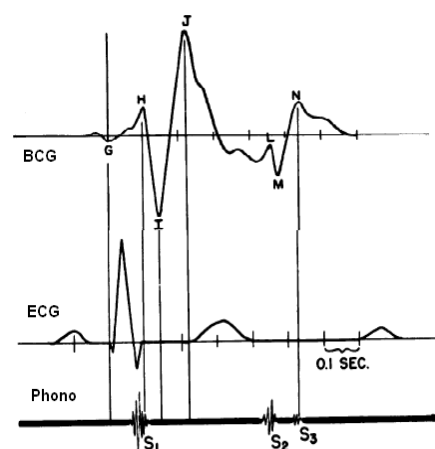

Fig. 2. Simulaneous BCG, ECG and Phonocardiograph signals (Scarborough & Talbot 1956)
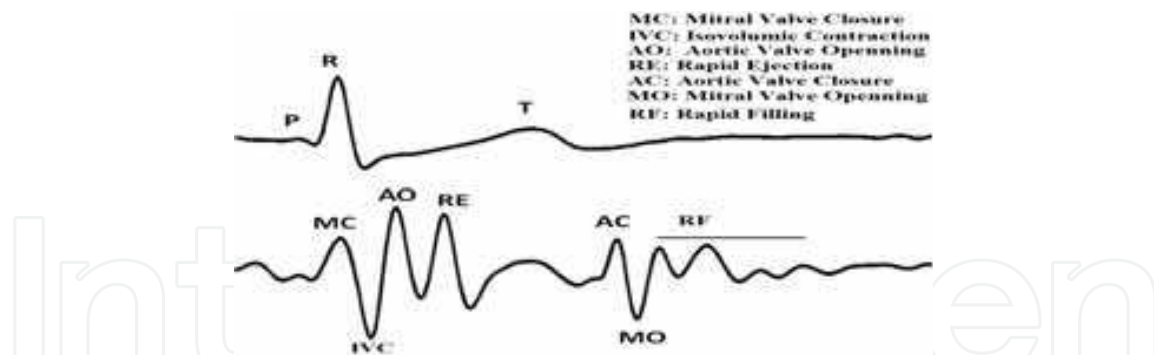
Fig. 3. A cycle of ECG (top) and SCG signals, from the second author, and the sequence of cardiac events assigned to it based on Salerno's research (Crow et al. 1994)

2.1.2 Seismocardiogram (SCG)

Seismocardiography is a technique used for analyzing the vibrations generated by the heart and it is recorded from the surface of the body using accelerometers. The seismocardiography was first introduced to clinical medicine by J. Zanetti (earthquake seismologist) and D. Salerno (cardiologist) in 1987. They borrowed the technology used in seismology to record the cardiac induced vibration from the surface of the body (Salerno & Zanetti, 1990a). This signal was also given the name Sternal Ballistocardiography as it was recorded from the sternum and had similarities to the ballistocardiogram (Mckay et al., 1999) (Tavakolian et al., 2008b). A cycle of synchronous SCG and ECG is shown in Fig. 3.

It was shown later on that changes in SCG after exercise was more sensitive for detection of moderate coronary artery stenosis than ECG. Later, the same claim was proven on more number of patients, 505, that the qualitative seismocardiography was more accurate, both in sensitivity and specificity, than electrocardiography for detection of coronary artery stenosis. This was true for severe, multivessle disease as well as for moderate disease and also for presence or absence of myocardial infarction (Salerno et al., 1990b).

There are two different subgroups of signals that have been introduced so far as seismocardiogram. In the first group, which consists the majority of the papers, the signal is recorded by positioning of an accelerometer on the sternum while in the second group other places on the torso such as left clavicle (Castiglioni et al. 2007) or hip (Trefny, 2005) were used. Thus, in a wider sense seismocardiogram is recording of cardiac induced vibrations on the upper part of the body while in a particular definition given by Salerno and his group seismocardiogram, is just limited to the vibration signals recorded from the sternum.

The first commercial SCG instrument was a failure as it required a heavy and bulky seismology sensor on the sternum which was cumbersome to tolerate for a long time. New sensor technologies have provided new possibilities for portable and wireless sensors that can be worn under clothing to record the SCG signal during daily activities. A new line of research has emerged aiming to re-introduce SCG as a clinical instrument that can be used to noninvasively and inexpensively diagnose cardiac abnormalities (Akhbardeh et al., 2007) (Castiglioni et al. 2007) (Tavakolian et al. 2008b).
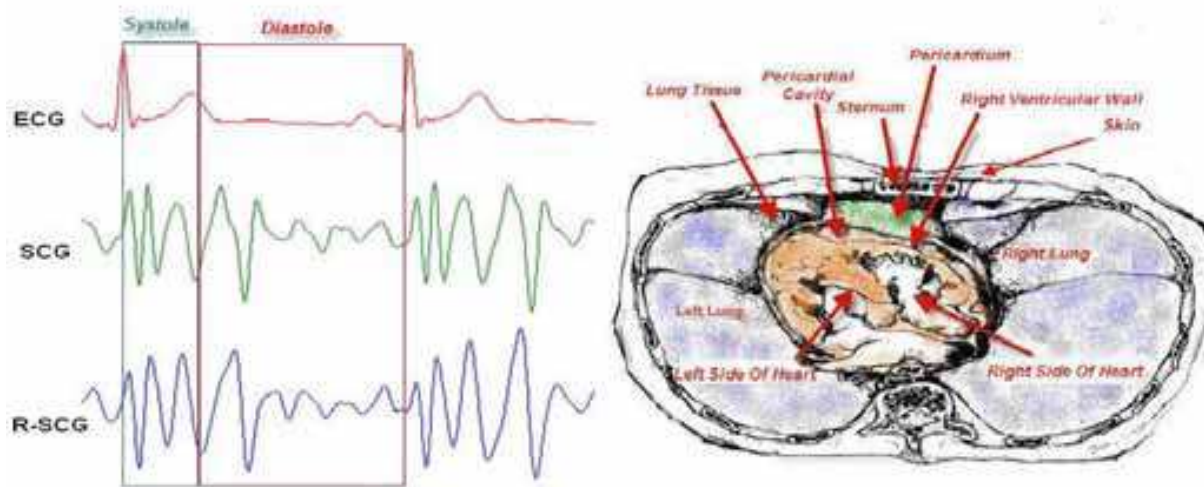
Fig. 4. Right: Positioning of different layers of tissues that the radar signal will go through. Left: two cycles of the R-SCG, SCG and ECG signals (Tavakolian et al., 2008a).

2.1.3 Radar seismocardiogram (R-SCG) and its Medical Relevance

Radar seismocardiogram also known as radarcardiogram (Geisheimer & Greneker, 1999) and mechanocardiogram (Tavakolian et al., 2008a) reflects the mechanical dynamics of the heart recorded by contactless methods. While monitoring the heart away from the chest the signal passes through only a few layers of different tissues between the sternum and the heart which can be seen in Fig.4. The tissue layers between the sensor and heart muscle include: skin, sternum, lung and pleural tissue, pericardium and pericardial space. From the sternum position these tissue layers are thinner compared to the other positions. Therefore, the best position to record the heart's R-SCG signal is from the sternum. R-SCG signal has close relationship to SCG signal as can be seen in Fig 4. In other words, proper processing of the radar signal reflected from the chest will enable us to extract a signal (R-SCG) which is very similar in morphology to SCG thus, a better understanding of SCG mechanism helps us understand R-SCG signal as well.

Some hemodynamic parameters can be extracted from either the amplitude or timings of R-SCG signal as can be seen in Fig. 5. The amplitude of R-SCG is an indication of the cardiac contractility thus, it is correlated with stroke volume and cardiac output (Mckay et al. 1999). The time intervals between the R-SCG peaks is correlated with cardiac intervals such as isovolumic contraction and relaxation times and ventricular ejection time. Calculation of these three cardiac intervals from R-SCG will provide us with the possibility of noninvasive calculation of a combined myocardial performance index called Tei-index.

Tei index equals isovolumic contraction time plus isovolumic relaxation time divided by ejection time. Congestive heart failure is related to contraction and relaxation abnormalities of the ventricle. Isolated analysis of either mechanism may not be reflective of overall cadiac dysfunction. Tei-index has been described to be more effective for analysis of global cardiac dysfunction than systolic and diastolic measures alone. Tei-Index is evaluated against

invasive examinations and proved to be a sensitive indicator of overall cardiac dysfunction in patients with mild-to-moderate congestive heart failure (Brush et al., 2000).
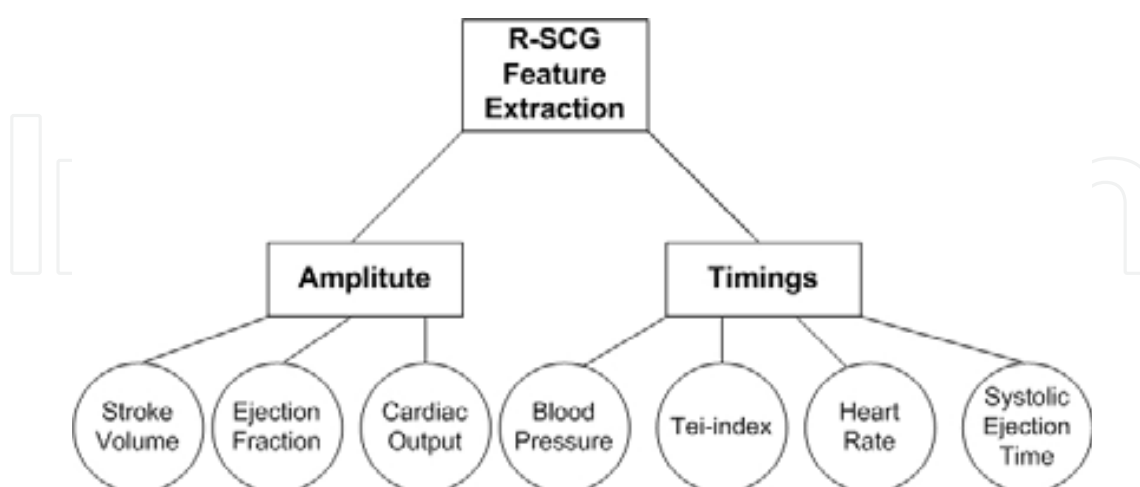

Fig. 5. Possible extraction of clinical parameters from R-SCG.

Vital signs are measures of various physiological statistics in order to monitors the most basic body functions. There are four standard vital signs: heart rate, respiratory rate, blood pressure and body temprature. Blood pressure is the pressure of the blood in the arteris and is created by the contraction of the heart. In clincs the blood presure is normally reported by two numbers. The higher number correponds to the systolic blood presure and is measured after the heart contracts and the other one is diastolic blood pressure and is measured befor the heart contraction.

Using R-SCG heart and breathing rates, can be reliably estimated. Further improvement of the current technolgy can enable us to estimate blood pressure from the R-SCG signal in future. The interval between the openning of aorta to the point of maximum systolic ejection is inversely proportional to the blood presure and can be used for the estimation of systolic blood pressure. In a novel study, from BCG signals acquired from bathroom scale, the interval between the R wave of ECG signal to the rapid ejection point of BCG was used for this estimation (Kim et al. 2006). Thus, except for temprature R-SCG can enable us to monitor three of the four vital signs as mentioned above.

2.1.4. Comparison Study of Infrasonic Cardiac Signals

As mentioned before, BCG signal is the most studied signal in the field of infrasonic cardiac signals and has been around for about a century. BCG is different compared to R-SCG and SCG as it reflects the movement of the center of gravity of the whole body and its support while the SCG and R-SCG signals reflect the mechanical vibration of the upper part of the body as recorded from its surface. Fig. 1. shows the differnt setups that were used for the acquistion of these signals.

The SCG and R-SCG signals are recorded from positions closer to the heart thus, there are less mechanical damping of the cardiac vibration compared to classical BCG in which, the

heart moves the whole body and the recording system (Bed, chair and weight scale). This finds more importance in the sense that, being close to the heart, SCG and R-SCG are able to trace valvular activities while these tiny movements gets dampen out by the classical BCG beds. Thus, in terms of evaluation of timings of valvular events SCG and R-SCG are a better reference compared to BCG.
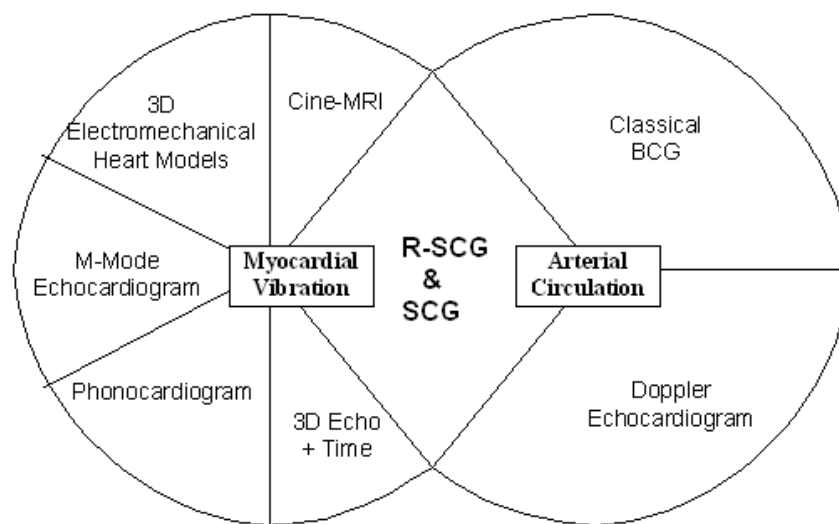

Fig. 6. The two main factors determining the R-SCG and SCG morphology and the possible tools for investigating them.

On the other hand, as BCG is a record of the sum of all the cardiovascular forces exerted on the body thus, its amplitude is a more faithful representation of the force of cardiac system compared to SCG and R-SCG which reflect a portion of this force that affects the upper body thus, BCG is a better candidate to estimate stroke volume and cardiac output compared to SCG. The old BCG instruments were quite bulky and required the patients to lie down on beds suspended from the ceiling while SCG and R-SCG facilitate signal recording and thus, provide alternative possibilities that BCG was inherently unable to.

Using R-SCG, on the other hand, provides a unique advantage, over other infrasoinc cardiac signals, that it does not require any mechanical contact to the body. Thus, in applications such as monitoring new born babies, to avoid sudden infant death syndrome (SIDS), R-SCG contactless recording is an advantage.

2.2. The Genesis of R-SCG waves

As mentioned previously the R-SCG morphology has close resemblance to SCG and it basically signals the same events in the cardiac cycle as SCG does. Thus, in this section, we briefly introduce different methods used for understanding of the genesis of SCG waves, assuming that this knowledge can be transferred to the R-SCG field as well.

The waves observed on R-SCG and SCG signals originate from two main cardiovascular phenomenons of myocardial contraction and arterial circulation. In other words, some components of the R-SCG are due to vibration waves directly created by the heart contractions and transferred to the surface of the body, and some other components are because of the recoil created by the circulation of blood in the arteries.

In a study conducted by Salerno the SCG signal was simultaneously recorded together with echocardiograph images for 39 subjects and it was shown that aortic and mitral valve opening and closures could be corresponded to peaks and valleys on the SCG signal (Crow et al. 1994). An example of SCG traces recorded in CiBER and annotated based on Salerno's work can be seen in Fig. 3. After the P wave on ECG and during the QRS complex there is a local maximum correpondig to the Mitral valve closure (MC) the interval between this point and the next maximum (The aortic valve opening) is the iso-volumic contraction interval. Rapid systolic ejection point (RE) is the next maximum after that, as it can also be identified in the Doppler echocardiogram on the left side of Fig.7 At the end of the sytole the aorta closes (AC) followed by the opening of the Miral valve (MO). The interval between AC and MO is defined as iso-volumic relaxation time.

The simultaneous echocardiogram and SCG and ECG signal used for investigation of cardiac events as recorded on the SCG signal can be seen in Fig. 7. On the left side of the figure by using Doppler echocardiogram and SCG; point of rapid systolic ejection is shown by a vertical red line in two consecutive cycles. On the right side of Fig. 7 the M-mode echocardiogram is shown and the aortic valve opening time is shown by a vertical green line and the aortic valve closure with a dotted blue line. The Echocardiograms were recorded in Burnaby General Hospital, Canada, using a GE vivid 7 system.

Echocardiograph is still the gold standard for investigation of the origin of the waves observed on R-SCG and SCG signals but there are two reasons to investigate for alternative solutions besides echocardiography. Firstly, echocardiography has limitations: being operator dependant, being dependant on the position of the transducer, and being limited to a few numbers of beats. Secondly, by using the Echo images alone we still do not clearly know how the underlying cardiac events create the waves observed on the signal recorded from the chest. The reason is the fact that these cardiac events superimpose on each other and sometimes amplify or decrease each other's effects. Thus, as can be seen in Fig. 6, other methodologies such as Cine-MRI and 3D, finite element, electromechanical model of the heart have been proposed to study the effect of cardiac contraction (Akhbardeh et al. 2009) and, on the other hand, classical BCG and Doppler echocardiogram have been proposed to study the effects of blood circulation on the SCG morphology (Ngai et al. 2009).

Phonocardiogram can also be used to study the effects of cardiac vibrations on the R-SCG morphology as can be seen in Fig. 10. The heart sounds as observed on phonocardiogram can be used to study the effects of valvular events on the morphology of the signal. Two cycles of synchronous radar R-SCG, Phonocardiograph and ECG signal showing the correlation of cardiac cycle events to R-SCG signal. Systolic and diastolic complexes can be identified in the radar R-SCG signal corresponding to S1 and S2 of heart sounds.
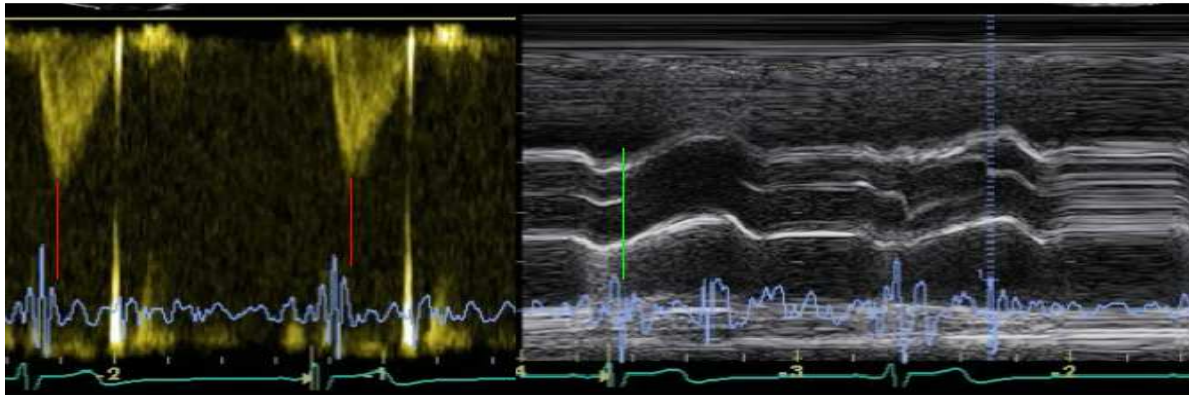
Fig. 7. left: Doppler echocardiogram and SCG; right: M-mode echocardiogram

2.3 Doppler Based Radar System

Radio detection and ranging (Radar) systems are used to identify the range, direction, or speed of both moving and fixed objects such as aircrafts, vehicles and terrains. These systems are usually comprised of an RF/Microwave transceiver to transmit the Electromagnetic signal to the object under test and receive the reflected wave carrying the required data. Depending on the application, this data is further processed using basic or advanced signal processing techniques. Microwave Doppler radar-based systems are one of the most common applications of radar in everyday life. These systems will be discussed in detail in Section 3.

A class of radars utilize Doppler Effect to measure the velocity of moving objects. This kind of approach has long been used to estimate the velocity of moving vehicles for speed control and other purposes. The Doppler principle has been used in different modalities including microwave, laser and ultrasound. Doppler radars are commercially used in air defence, air traffic control, sounding satellites, and even police speed guns.

Microwave electromagnetic waves can propagate through the body and are reflected at the interfaces between different tissue layers. By the Doppler Effect for Microwave radar, if a radio frequency wave is transmitted to a moving surface, the reflected wave undergoes a frequency shift proportional to the surface velocity. If the surface has periodic motion, like that of the heart and chest, this can also be seen as a phase shift proportional to the surface displacement. If this displacement is small compared to the wavelength, a low-frequency component can be extracted from downconversion and filtering (removing the high-frequency component) the reflected wave that is directly proportional to the object displacement.

The Doppler Effect can be written as (Skolnik, 1990):

$$\omega_r = \omega_0 (1 + \frac{v}{c} Cos\alpha) \tag{1}$$

where ω_r corresponds to the reflected wave frequency, ω_0 corresponds to the transmitted wave frequency, v corresponds to the relative speed, c corresponds to the prorogation speed of the wave (in this case, the Electromagnetic wave speed which is 3×10^8 *m/s* in free space)

and finally, *a* corresponds to the angle of the reflected wave versus the moving object. If the transmitter and the moving object are approaching each other, then the reflected wave frequency is higher than the transmitted wave frequency ($\omega_r > \omega_0$) and if they are departing from each other, then the reflected wave is lower than the transmitted wave frequency ($\omega_r < \omega_0$). Assuming the transmitted wave direction to be along the movement direction of the object under test (*a=0*), the Doppler Effect for a return way can be re-written as:

$$\omega_r = \omega_0 + \omega_D = \omega_0(1 + \frac{2v}{c}) \tag{2}$$

Therefore, the speed of the moving object can be calculated. The operation of the Microwave radar based systems will be further analysed in Section 3.3.

2.4 The Ultra-wideband (UWB) Radar for Biomedical Applications

In 2002, the Federal Communications Commission (FCC) allocated the 3.1 to 10.6GHz band to ultra-wideband (UWB) communication systems in which the systems have a bandwidth greater than 500MHz and a maximum equivalent isotropic radiated power (EIRP) spectral density of −41.3dBm/MHz (FCC, 2002). This broad definition has encouraged a variety of UWB variants for different applications including UWB Doppler radar for vital signal sensing (Staderini, 2002a). UWB power levels are very low and therefore reduce the risk of molecular ionization (Jauchem et al., 1998). In addition, advances in modern silicon integration technologies with high cutoff frequencies allow for small, low-power implementation of UWB sensors. Time-gating of short radar UWB pulses allows for additional power efficiency; however, as explained in section 3.2., new design challenges on the control of sampling at the receiver is introduced.

Doppler radar-based systems for cardiovascular and respiratory measurements date back to the late 1970's and early 1980's for the X-band (around 10GHz) (Lin, 1975; Lin, 1979; Chen et al., 1986). In mid-1980s, a frequency-modulated-continuous wave (FM-CW) system was developed to detect the vital signs of a wounded soldier in live fire situations at distances of up to 100 meters (Greneker, 1997). Despite its severe limitations such as sensitivity to surrounding objects, this device was the first of the many later developed radar vital signs monitor (RVSM) devices (Thansandote et al., 1983).

RVSM devices are capable of detecting human heart beat and respiration rate in a contact-less manner, by transmitting a radio frequency signal to the subject and measuring the phase shift in the reflected signal based on the Doppler Effect. During the 1996 Olympics, a variant of the RVSM, developed by Georgia Tech Research Institute (GTRI), (Greneker, 1997), was developed for assessment the performance of the athletes in the archery and rifle competitions. Human heartbeat and respiration signals were measured at ranges exceeding 10 meters using this RVSM that was mounted onto a 0.6m parabolic dish antenna and transmitted an output power of 30mW at 24.1 GHz. Other suggested applications for these devices include home telemedicine monitoring systems and security applications. Major problems with these devices include sensitivity to surroundings due to weak signal processing and their high cost due to bulkiness.

In (Thansandote et al., 1983), a microwave Doppler radar system was reported for continuously monitoring time-varying biological impedances. The radar compares the phase of the signal scattered from the biological tissue with that of the transmitted signal.

The phase variations of the scattered signal are indicate the net impedance changes in the test region due to physiological processes, e.g. movements of blood vessels during the cardiac cycle. The system operation at both frequencies of 3GHz and 10.5GHz was tested with healthy human subjects. The 3GHz operation frequency for the Doppler radar system was shown to have significantly greater penetration in tissues but was less sensitive to changes of the biological impedance than the 10.5GHz system.

A simple add-on module was reported in (Lubecke et al., 2002) that allows the Doppler radar based detection of human respiration and heart activity using the 2.4 GHz cordless telephone system without requiring modifications in the existing telephone infrastructure. This module includes an inverted F-type antenna combined with a Schottky diode as the mixing element. The implemented module is very small in size but does not implement the complete system and the receiver baseband section is implemented on a digitizing oscilloscope.

A digital signal processor was described in (Lohman et al., 2002) for the determination of respiration and heart rates in Doppler radar measurements for remote monitoring. The processor can reliably calculate both rates for a subject at distances of 2m. Several enhancement techniques such as autocorrelation and center clipping are used. The calculated heart rates agree for over 88% of the cases, within a 2% margin, for all datasets.

The first single-chip radios for the remote sensing of vital signs using direct-conversion radars integrated in low-cost silicon technologies were implemented in (Droitcour et al., 2001). Two Doppler radar systems operating at 1.6GHz were fabricated using CMOS/BiCMOS technologies with more than 83% agreement with references. Despite the high phase noise of the integrated oscillators, heart and respiration rates were detected remotely, using phase noise reduction through range correlation (Droitcour et al., 2001).

In (Thijs et al., 2005), the data obtained from a commercially available continuous-wave Doppler radar sensor (KMY24) was compared to an ICG device using a Cardiac Output Monitor (Medis Niccomo). The obtained data was shown to be clearer on the captured radar signal than on the ICG, for example, the opening of the atrium and the mitral valve (Thijs et al., 2005).

An infant vital sign monitor device is reported in (Li et al., 2009). This device operates at 5.8 GHz and monitors the existence of the infant's heart and respiration rate. Therefore, the signal processing required for this device is simplified.

Several UWB Microwave Doppler radar based implementations have also been reported in the literature based on (McEwan, 1994). A bread-board UWB prototype is implemented in (Michahelles et al., 2004) that can determine the heart-rate at a distance of up to 15cm with a relative error of 5% compared to oximeter measurements.

Another UWB prototype was developed in (Staderini, 2002b) using a dipole antenna that emits 2ns pulses with a mean pulse repetition frequency (PRF) of 2MHz. This prototype is used to measure the HRV signal. Using fast Fourier transform (FFT), the spectral content of the radar captured signal is compared to an ECG-derived HRV signal and good correlations are confirmed.

UWB radar systems have also been reported to detect human beings behind walls Meyerhoff, 2007), or as lie detectors (Staderini, 2002b), or as human activity monitoring, e.g., detection of walking, running, sleeping, etc., (Dutta et al., 2006; Such et al., 2006; Chia et al., 2005) using the body signals.

A system-on-chip (SoC) implementation of a UWB vital signal sensor is in progress funded by the European Union (Zito et al., 2007; Zito et al., 2008). In this project, a wearable UWB radar wireless sensor for detection of heart and breath rates is to be implemented using CMOS 90nm technology. Short pulses of 200-300ps duration with a PRF of 1-10 MHz are used (Zito et al., 2008). An IEEE 802.15.4 ZigBee (ZigBee Alliance, 2004) low-power radio interface is used for wireless data communication.

3. The Microwave Doppler-Based Radar System Blocks and Specifications

A block diagram depicting the main blocks of the Microwave Doppler-based radar system is shown in Fig. 8. As shown in this figure, these devices are generally composed of two main stages: The RF stage and the baseband signal processing stage. The RF stage includes an RF/UWB transceiver block to transmit the radar wave and receive the reflected wave. The received wave includes the frequency shift due to the motion/velocity of the target (e.g. thorax, blood flow). The received signal is down-converted and low-pass filtered to extract the baseband shifting data. This baseband signal is further amplified, digitized, and processed in the baseband stage. The digital signal processing techniques can be implemented in hardware or software.

In this section, the Doppler based Radar system is analyzed, the main stages as shown in Fig. 8 are reviewed, and some major reported ideas for on-board and CMOS integrated implementation of these blocks are discussed.

3.1 The RF Stage

As shown in Fig. 1, on the transmit side, the RF stage includes a pulse generator (Gaussian pulse, in case of UWB system), a mixer (LO) to modulate the pulse, a power amplifier (PA) to radiate the modulated pulse, and finally a transmitting antenna. The transmitted signal can be a continuous wave monochrome (single frequency) non-modulated sinusoidal radar signal. In this case the system is simplified to the non-dashed blocks and only the signal generated at the LO is transmitted (no pulse generator or mixer stage required).

On the receive side, the reflected beams are captured by the receiving antenna, followed by a low-noise amplifier (LNA), a downconversion mixer, and a low-pass filter. The downconversion mixer multiplies the received signal by a replica (a delayed replica if time-gating is used) of the same signal as the one at the transmit side to demodulate it. The signal is then filtered to extract the low frequency component that includes the shift depending on the object motion data. Similar to the transmit side, if monochrome radar is used, no downconversion mixer stage is required.

The choice of a proper frequency is a compromise and depends on the test objectives, as a higher frequency enables a larger Doppler shift and therefore a higher resolution, but also results in a lower tissue penetration depth. In many reported works, the 2.45GHz frequency is chosen to exploit the commercially available components, e.g. (Lubecke et al., 2002). The frequency of the transmitted beam is adjusted by the mixer signal provided by the local oscillator (LO) block. The LO signal can be a voltage controlled oscillator (VCO) or simply a crystal oscillator. In the case of UWB radar systems, a short Gaussian monopulse is generated with a pulse-width in the order of magnitude of a few nanoseconds. Several short pulse generators have been reported in the literature. For example, digital pulse generators

have been suggested in (Wentzeloff & Chandrakasan, 2006), for on-chip or on-board implementation based on a short delay between two NAND gates.
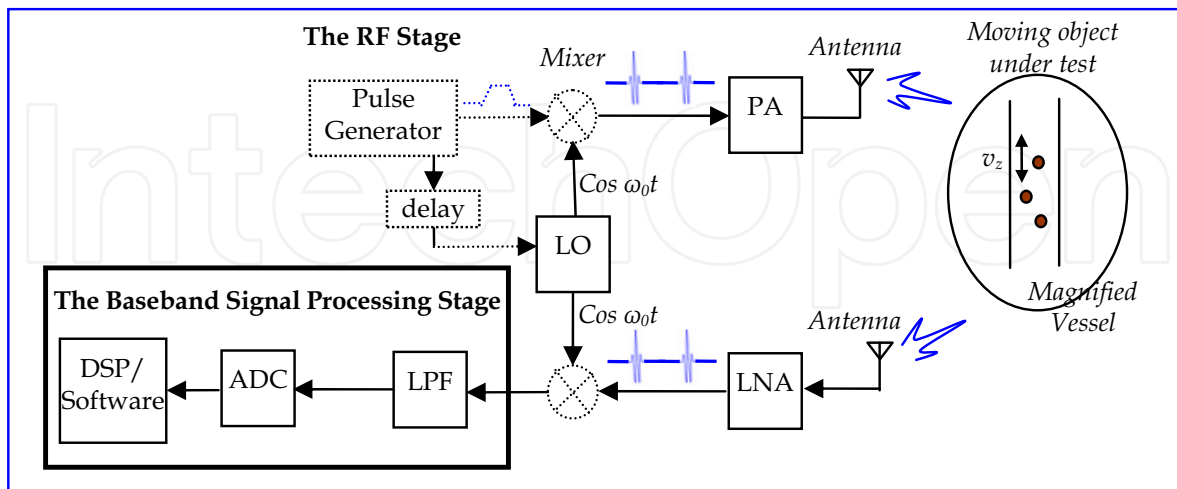

Fig. 8. The Microwave Doppler Radar-based system block diagram

The modulated signal is amplified by the PA and propagated by the transmitting antenna. In (Zito et al., 2008), a system-on-chip UWB sensor is implemented using a shaper block for the mixer and an integrator to sample and low-pass filter the received signal. In (Prak et al, 2007), quadrature mixers are used for the modulation/demodulation stages to increase accuracy and arctangent demodulation and dc-cancellation methods are used.

3.2 Time-Gating

To reduce power, in particular where battery-operated wireless handheld devices are implemented, the same antenna and mixing stage can be time-gated between the transmitting and the receiving stage. For example, by assigning a 50% duty cycle to a generated square pulse, the system can transmit the illuminating monochrome signal for the first half of the pulse width and receive the reflected signal for the second half of the pulse width. Note that in this case the dashed blocks are used in Fig. 1. A switch or a circulator can be used to implement the time-gating with the desired time-span.

UWB short-pulse systems are usually implemented using this structure and pulses as short as a few nanoseconds are used. As shown in Fig. 1, the pulse generator also activates a delay line block. This block controls proper sampling of the received signals from the object. The receiver only samples at short time intervals triggered by the delay line block. Proper timing of this triggering is essential to ensure sampling only when the received signals from a certain distance are received, for example, only when echoes of the heart-wall are expected (Michahelles et al., 2004). Intuitively, this delay should be equal to the flight time of the pulse from the radar to the heart and then from the heart to the radar. Note that time gating and adjusting the sampling time increases the signal-to-noise-ratio at the receiver as less interference signals due to body movements and other moving objects are sampled. Therefore, the effect of the interferences is less pronounced.

Time-gating is specified by the pulse repetition frequency (PRF). The PRF is defined as the number of pulses transmitted per second. It should be noted that depending on the velocity

of the object under test and the application, a minimum PRF should be met that depends on the radar range and the speed of the radar waves (in this case, *c*, for electromagnetic waves). To avoid ambiguity and increase the velocity measurement accuracy, sufficient observation time is required, which is possible by choosing proper PRF (Skolnik, 1990).

3.3 Analysis

For simplicity and without loss of generalization, assume a monochrome continuous RF-modulated signal, *x(t)*, is chosen as the radar transmitting signal:

$$x(t) = A \cdot Cos(\omega_0 t) \tag{3}$$

The reflected signal captured at the receive side will include the transmitted signal provided by the signal generator, with a frequency shift, ω_d, that is proportional to the velocity of the blood flow. The received signal will therefore include a term:

$$y(t) = A \cdot Cos[(\omega_0 + \omega_d)t] \tag{4}$$

plus some noise terms, where,

$$\omega_d = \frac{2v\omega_0}{c} \tag{5}$$

where ω_0 is the mixer frequency, *c* is the speed of light, and *v* is the velocity of the moving object under test; for example blood-flow velocity in arteries and veins, or the heart wall.
The frequency displacement resulting from the motion of the object under test can also be modelled as a phase shift, $\Phi(t)$, that depends on the velocity: (Thijs et al., 2005; Thansandote et al., 1983; Lohman et al., 2002)

$$\Phi(t) = \frac{2\pi}{\lambda} \int_0^t v(\tau)d\tau = \frac{4\pi}{\lambda} s(t) \tag{6}$$

where λ is the wavelength and *s(t)* is the movement amplitude. Therefore, the vital signals such as the movement of the Thorax can be sensed.
In the case of UWB radar, the transmitted signal would be the product of a narrow Gaussian pulse by the mixer signal:

$$x(t) = Cos(\omega_0 t) \cdot \sum_{n=0}^{\infty} \exp\left[-\frac{(t - \mu - nT_p)^2}{2\sigma^2} \right] \tag{7}$$

and the reflected, received signal will include the Doppler shifted component,

$$y(t) = Cos(\omega_0 + \omega_d)t \cdot \sum_{n=0}^{\infty} \exp\left[-\frac{(t - \mu - nT_p)^2}{2\sigma^2} \right] \tag{8}$$

where ω_0 is angular frequency of UWB modulation signal, ω_d is the Doppler shift frequency, μ represents Gaussian envelope phase, σ represents the pulse width and T_p is the pulse repetition period (corresponding to the PRF). Here, the added noise components not taken into account.

To extract the velocity of the object under test from the received signal, *y(t)* is downconverted by *Cos(ω₀t)*, as (ignoring the mismatch errors)

$$y(t) = Cos((\omega_0 + \omega_d)t) \cdot Cos(\omega_0 t) \sum_{n=0}^{\infty} \exp\left[-\frac{(t - \mu - nT_p)^2}{2\sigma^2} \right] \qquad (9)$$

That can be rewritten as:

$$y(t) = \left[Cos((2\omega_0 + \omega_d)t) + Cos(\omega_d t) \right] \cdot \sum_{n=0}^{\infty} \exp\left[-\frac{(t - \mu - nT_p)^2}{2\sigma^2} \right] \qquad (10)$$

Therefore, the high frequency component can be filtered and the remaining baseband term that includes the shift data, i.e.,

$$y(t) = Cos(\omega_d t) \cdot \sum_{n=0}^{\infty} \exp\left[-\frac{(t - \mu - nT_p)^2}{2\sigma^2} \right] \qquad (11)$$

is transferred to the following baseband signal processing stage.

3.4 The Baseband Stage

The baseband signal processing stage is the last stage in the Microwave Doppler radar-based system. In this stage, the frequency shift data and therefore the velocity/motion rate of the object under test is extracted from the signal received at the output of the lowpass filtering stage. Depending on the application, the received signal is processed through various digital signal processing (DSP) techniques. Usually, the received signal at the baseband stage is first amplified and converted into digital by an analog-to-digital converter stage (ADC) and then processed by further DSP techniques in the digital domain, where more flexible, simpler, and potentially lower cost implementations are possible. DSP techniques in the time-domain or frequency-domain such as fast Fourier transform (FFT), autocorrelation and noise cancellation methods, as well as several digital filtering stages can be used to increase coherency, attenuate the noise terms (such as echo), cancel motion artefacts due to other movements in the body and surrounding objects, and extract the target data.

The DSP techniques can be implemented in hardware (board-level or integrated), or in software, using a PC (e.g. MatLab™ DSP toolbox), or both, depending on the application. The DSP blocks can be implemented in hardware, on an FPGA, or on a DSP module, depending on their complexity. Also, several DSP prototype development boards are available by Texas Instruments Inc., and Altera Co. that can accommodate various applications.

In order to select proper hardware for a specific application, requirements on the maximum measurement frequency and resolution should be decided. Body signal such as blood flow rate or heart rate are usually not high frequency and therefore the requirements are not tight. However, some applications may require better resolutions. The Nyquist-rate requirement for proper sampling by the ADC is specified as:

$$f_s \geq 2f_{max} \tag{12}$$

where f_{max} is the maximum measurement frequency and f_s is the sampling frequency of the ADC. Oversampling can help increase the signal-to-noise-ratio (SNR) and therefore the resolution of the digitized signal (Northworthy et al., 1996). Note that these two parameters are related as (Northworthy et al., 1996):

$$SNDR = 6.02n + 1.76 \, dB \tag{13}$$

where n is the effective number of bits (ENOB) of an ADC, known as the resolution of the ADC. As an example, in case of the heart signals measurements, a baseband signal of less than 30 Hz is expected at the output of the RF stage, therefore a sample rate of 80-100Hz for the ADC would be required.

4. The Developed R-SCG System and Measurement Results

The principal design of the radar-based R-SCG device is shown in the block diagram of Fig 9. The antenna mounted on the device is HFMD24 by Siemens and contains a transmitter and a receiver in the same housing. The operating frequency is 2.45GHz. The transmitter transmits continuous wave radio frequency energy towards subject body. The output signal from the receiver is filtered and amplified, signal conditioning block. The cut-off frequencies for the band-pass filter are 1Hz and 100Hz and the gain of the amplifier is around 800. After filtering and amplifying, the R-SCG signal is sent to the A/D unit and then to the ATMEL CPU for further processing. The CPU is connected to a thin-film transistor (TFT) display via its SPI (Serial Peripheral Interface) port. The R-SCG device operates with two AA batteries (2.45V) (Tavakolian et al, 2008a).

Considering that the R-SCG device has its own CPU and monitor, it can be used stand alone to acquire and process the R-SCG signal. There is also another option of sending the data to a personal computer for more advanced processing of the data using Matlab. To have this option on our device, the digitized R-SCG signal is transformed to packets and sent through UART to the USB and finally to the host personal computer for possible further processing.
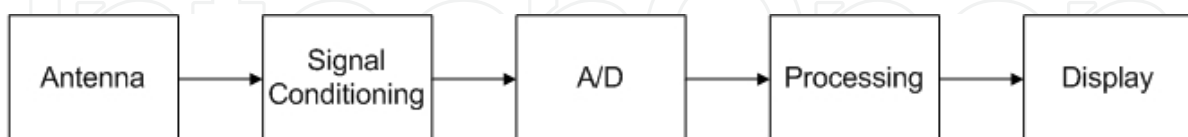

Fig. 9. Block diagram of the R-SCG device

The R-SCG signal was acquired by the sensor, 10cm away from the subject chest. The data acquisition involved the measurement of ECG and respiration signals too. RF signal with the carrier frequency of 2.45 GHz was transmitted toward the subject's chest and the reflected signal was band-passed filtered between 0.5 to 25 Hz. The filtered signal was differentiated and then band-pass filtered again between 4 Hz to 20 Hz. The comparison of the processed R-SCG signal to the SCG signal recorded simultaneously from the sternum can be seen in Fig. 4 together with the synchronized ECG signal.

It can be observed that there is a close correlation between the signal acquired from the radar-based R-SCG device and the simultaneous signal recorded from the SCG sensor attached to the sternum. The systolic and diastolic phases of cardiac cycle are shown to identify the correlations of these mechanical signals to the heart functioning. As explained before in section two, due to this close resemblance of the signal to SCG we are able to transfer the knowledge in the SCG field, about the genesis of waves, to R-SCG analysis.

Phonocardiograph signal reflects the heart sounds that can be hared using stethoscope. Heart sound S1 corresponds to systolic phase of the heart cycle and S2 corresponds to the diastolic phase of it. For the comparison purpose, the R-SCG signal was acquired synchronously with phonocardiogram signal and it was observed that S1 and S2 sounds of the phonocardiograph signal corresponded to the similar complexes on the R-SCG displacement signal as can be seen in Fig.10.

The data from subjects were recorded at Burnaby General Hospital. For the heart rate measurement the experimental setup included the acquisition of the R-SCG signal and two leads of ECG as a reference. For respiration rate measurement the setup included the acquisition of R-SCG signal together with the respiration signal as the reference. Eight subjects took part in the respiration measurement tests and six of these subjects took part in the heart rate measurement tests too. Breathing rate measurement experiments were 60 seconds long while heart rate measurement experiments were 15 seconds long.

For detection of breathing rate the radar signal was low pass filtered under 0.4Hz and the peaks were counted and compared to the results acquired from a strain gauge transducer that measures the changes in thoracic circumference, using a belt which is fastened to the subject's thorax. The accuracy of respiration rate measurement was 91.35 percent over all eight subjects. The heart rate was measured using radar-based R-SCG device and was compared to the heart rate calculated from the simultaneous ECG signal for six subjects. The average of the heart rate accuracy on these subjects was calculated to be 92.9 percent.

4.1 Safety Issues

In order to standardize and commercialize the developed device, the radar sensor's SAR (specific absorption rate) should be determined. SAR measurements are usually used for cellphone handsets to assess the thermal effect on the human body tissue due to cellphone radiation. It is also a measure of the amount of energy absorbed by the human body. The SAR value for similar sensors have been measured to be lower than a standard cellphone handset (Thijs et al., 2005).
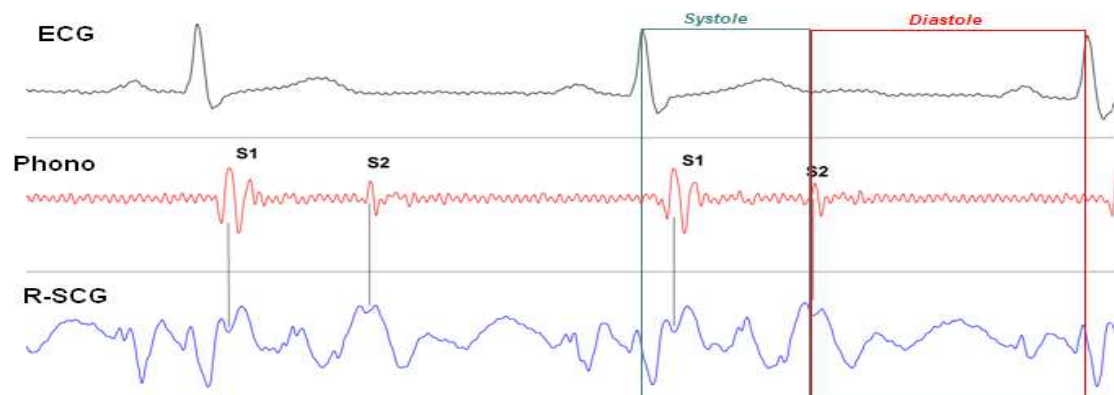
Fig. 10. Synchronous radar displacement R-SCG, Phonocardiograph and ECG signals (Tavakolian et al, 2008a)

5. Concluding Remarks and Future Work

Microwave Doppler radar-based systems can be used to monitor vital signs such as heart and breathing rate and to extract Radar seismocardiogram, by which, several other cardiac dynamic parameters can be estimated. Thus, in this chapter, a brief review of reported devices using continuous-time, and Ultra-wideband Microwave Doppler radar is presented as the technical basis of R-SCG device. Basic system design and implementation criteria are discussed and measurement results are shown. As an example, a system developed in the Simon Fraser University is discussed. On the other hand, the category of infrasonic cardiac signals has been investigated to further clarify the possible application of the recorded R-SCG signal in estimation of hemodynamic parameters.

Preliminary studies and measurements confirm that these systems can also be used to monitor cerebral blood flow, arterial blood flow and blood flow in bones. Compared to the conventional ultrasound methods, Microwave Doppler radar offers the advantage of ability to detect blood flow under bony tissues. A feasibility analysis for measuring cerebral blood flow using Microwave Doppler radar based devices can be found in (Jalali Mazlouman et al., 2009).

Although there are a variety of applications for vital signals monitoring where movement is not an issue, such as avalanche victims, and wireless monitoring of patients in a hospital or the elderly overnight, future work should focus on methods to detect and classify body movements, as also recommended in (Michahelles et al., 2004). For this purpose, more elaborate signal processing methods can be used to decrease the effects of the motion artefacts due to other body motions or movements of objects in the surrounding (Morgan & zierdt, 2009). To name a few, multiple antenna methods are recommended in (Li et al., 2009), to eliminate the noise caused by random body movements and clutter. A more recently used parametric and cyclic optimization algorithm, referred to as RELAX algorithm is suggested in (Li & Stocia, 1996) for spectral analysis of the captured signals. Blind source separation techniques using direct conversion Doppler radar and multiple antennas are recommended in (Vergara et al., 2008) to suppress the effect of other body motions and to capture real-time

Cardiopulmonary signals. Random body movement cancellation methods using complex quadrature demodulation and arctangent demodulation techniques are presented in (Li & Lin, 2008).

6. Acknowledgement

We would like to thank Alireza Akhbardeh and Brandon Ngai for helping us in preparation of this chapter.

7. References

Akhbardeh, A.; Junnila, S.; Koivuluoma, M.; Koivistoinen, T.; Turjanmaa, V. Kööbi, T.; Värri, A. (2007) Towards a Heart Disease Diagnosing System based on Force Sensitive chair's measurement, Biorthogonal Wavelets and Neural Network classifiers. *Engineering Applications on Artificial Intelligence*, Vol. 20, Issue 4, pp. 493.

Akhbardeh, A.; Tavakolian, K.; Gurev, V.; Lee, T.; New. W.; Kaminska, B.; Trayanova, N. (2009). Comparative Analysis of Three Different Modalities for Characterization of the Seismocardiogram" submitted to *31st IEEE Engineering in Medicine and Biology conference 2009*.

Bruch, C.; Schmermund, A.; Marin, D.; Katz, M.; Bartel, T.; Schaar, J.; Erbel, R; (2000). Tei-Index in patients with mild-to-moderate congestive heart failure. *European Heart Journal* (2000) 21, 1888–1895.

Castiglioni, P.; Faini, A.; Parati, G.; Rienzo, M.D. (2007). Wearable Seismocardiography. 29th IEEE EMBS, Lyon, France, August 2007, pp 3954-3958.

Chen, K.; Misra, D.; Wang, H.; Chuang, H. & Postow, E. (1986). An X-Band Microwave Life-Detection System. *Biomedical Engineering, IEEE Trans.*, BME-33, no.7, pp.697-701, July 1986.

Chia, M. Y. W.; Leong, S. W.; Sim, C. K. & Chan, K. M. (2005). Through-wall UWB radar operating within FCC's mask for sensing heart beat and breathing rate. *Microwave Conf., European*, Vol.3, pp. 4-6, Oct. 2005.

Crow, R.S.; Hannan, P.; Jacobs, D.; Hadquist, L. Salerno D.M. (1994). Relationship between Seismocardiogram and Echocardiogram for Events in Cardiac Cycle., *American Journal of Noninvasive Cardiology*, Vol. 8, pp.39-46, 1994.

Droitcour, A.; Lubecke, V.; Jenshan Lin & Boric-Lubecke, O. (2001). A microwave radio for Doppler radar sensing of vital signs. *Microwave Symp. Digest, 2001 IEEE MTT-S Int.*, Vol.1, pp.175-178, 2001.

Dutta, P.K.; Arora, A.K.& Bibyk, S.B. (2006). Towards radar-enabled sensor networks. *5th Int. Conf. on Information Processing in Sensor Networks (IPSN)*, Nashville, Tennessee, USA, April 2006.

FCC (2002), Federal Communications Commission, *Revision of part 15 of the commission's rules regarding ultra wideband transmission systems*. April 2002, www.fcc.gov/Bureaus/Engineering _Technology/Orders/2002/fcc02048.pdf.

Greneker, E.F. (1997). Radar Sensing of Heartbeat and Respiration at a Distance with Applications of the Technology, *IEEE Conference on Radars*, UK, pp 150-154, 1997.

Geisheimer, J.; Greneker, G. (1999). Applications of neural networks to the radarcardiogram (RCG), SPIE Conference on Applications and Science of Computational Intelligence Orlando, Florida, April 1999, SPIE Vol. 3722.

Heart and Stroke (2004), http://www.heartandstroke.com/site/c.ikIQLcMWJtE/ b.3483991/k.34A8/Statistics.htm#heartdisease

Inan, O.T.; Etemadi, M.; Wiard, R. M.; Kovacs, G. T. A. & Giovangrandi, L. (2008). Non-Invasive Monitoring of Valsalva-Induced Hemodynamic Changes Using a Bathroom ScaleBallistocardiograph," *30th Annual IEEE Engineering in Medicine and Biology Conference*, Vancouver, B.C., August, 2008.

Jalali Mazlouman, S.; Mahanfar, A. & Kaminska, B. (2009). Contact less Monitoring of the major blood vessels supplying head and brain (Carotid Arteries). *Nanotech09*, Houston, Texas, May 2009.

Jauchem, J.R.; Seaman, R.L.; Lehnert, H.M.; Mathur, S.P.; Ryan, K.L.; Frei, M.R. & Hurt, W.D. (1998). Ultra-wideband electromagnetic pulses: lack of effects on heart-rate and blood pressure during two-minute exposures of rats. *Bio-electromagnetics*, vol. 19, No. 5, pp. 330-333, 1998.

Jensen, B.H.; Larsen B.H. & Shankar,K. Monitoring of the Ballistocardiograph with the Static Charge Sensetive Bed (1991). *IEEE Transaction on Biomedical Engineering*, Vol. 38, No. 8, August 1991.

Junnila, S.; Akhbardeh, A. & Värri, A. (2008). An Electromechanical Film Sensor Based Wireless Ballistocardiographic Chair: Implementation and Performance, Journal of Signal Processing Systems, Springer New York, pp. November 11, 2008

Kim, J.S.; Chee, Y.J.; Park, J.W.; Choi, J.W.; Park, K.S. (2006). A new approach for non-intrusive monitoring of blood pressure on a toilet seat. *Journal of Physiological Measurement*, Institute of Physics 27 (2006) 203–211.

Li, C. & Lin, J. (2008). Random Body Movement Cancellation in Doppler Radar Vital Sign Detection, *Microwave Theory and Techniques, IEEE Trans.*, Vol.56, No.12, pp.3143-3152, Dec. 2008.

Li, C.; Cummings, J.; Lam, J.; Graves, E. & Wu, W. (2009). Radar Remote Monitoring of Vital Signs. *Microwave Magazine, IEEE*, Vol.10, No.1, pp.47-56, Feb. 2009.

Lin, J.C. (1975). Non-invasive Microwave Measurement of Respiration, *Proceedings of the IEEE*, vol. 63, pp. 1530, 1975.

Li J. & Stoica, P. (1996). Efficient mixed-spectrum estimation with applications to target feature extraction, *Signal Processing, IEEE Trans.*, Vol.44, No.2, pp.281-295, Feb 1996.

Lin, J.C.; Kiernicki, J.; Kiernicki, M. & Wollschlaeger, P.B. (1979). Microwave Apexcardiography, *Microwave Theory and Techniques, IEEE Trans.*, vol.27, no.6, pp. 618-620, Jun 1979.

Lohman, B.; Boric-Lubecke, O.; Lubecke, V.M.; Ong, P.W. & Sondhi, M.M. (2002). A Digital Signal Processor for Doppler Radar Sensing of Vital Signs. *IEEE Engineering in Medicine and Biology*, 2002.

Lubecke, V.; Boric-Lubecke, O. & Beck, E. (2002). A compact low-cost add-on module for Doppler radar sensing of vital signs using a wireless communications terminal. *Microwave Symp. Digest, IEEE MTT-S Int.*, Vol.3, pp.1767-1770, 2002.

McEwan, T. E. (1994). Ultra-wideband radar motion sensor.*US Patents* #5361070, 1994.

McKay, W.P.S.; Gregon, P.H.; McKay, B.; Militzer, J; (1999) Sternal Acceleration Ballistocardiography and Arterial Pressure Wave Analysis to Determine Stroke Volume. Clin Invest Med; 22(1), pages 4-14, 1999.

Meyerhoff, N.J. (2007). Intrusion Detection by Ultra-Wide Bandwidth Radar. *Technologies for Homeland Security, IEEE Conf.,* pp.81-84, 16-17 May 2007.

Michahelles, F.; Wicki, R. & Schiele, B. (2004). Less contact: Heart-rate Detection Without Even Touching the User, *Proceedings of Wearable Computers* (*ISWC 2004*) *8th Int. Symp.*, vol.1, pp. 4-7, 31 Oct.-3 Nov. 2004.

Morgan, D.R. & Zierdt, M.G. (2009). Novel Signal Processing Techniques for Doppler Radar Cardiopulmonary Sensing, *Signal Processing J.*, Vol. 89, No.1, Jan. 2009, pp. 45-66, ISSN 0165-1684, DOI: 10.1016/j.sigpro.2008.07.008.

Norsworthy, S. R.; Schreier, R., & Temes G. C. (1996). *Delta-Sigma Data Conversions*, Wiley-IEEE Press, ISBN: 978-0780310452.

Ngai, B.; Tavakolian, K.; Akhbardeh, A.; Blaber, A.P.; and Kaminska, B. Comparative Analysis of Seismocardiogram Waves with the Ultra-Low Frequency Ballistocardiogram. Submitted to 31st *IEEE Engineering in Medicine and Biology conference 2009*.

Park, B.K.; Boric-Lubecke, O.; Lubecke, V.M. (2007). Arctangent Demodulation With DC Offset Compensation in Quadrature Doppler Radar Receiver Systems, *Microwave Theory and Techniques, IEEE Trans.*, Vol.55, No.5, pp.1073-1079, May 2007.

Salerno, D.; Zanetti, J. (1990a). Seismocardiography: A new technique for recording cardiac vibration. Concept, method and initial observation", *J Cardiovasc Technol*, Vol. 9, pp. 111–117, 1990.

Salerno, D.; Zanetti, J.; Green, L. (1990b). Qualitative exercise seismocardiography for detection of moderate and severe multivessel coronary artery disease. *J Am Coll Cardiol* 1990; 15:44A.

Scarborough, W.R.; Talbot, S.A. (1956) proposal for ballistocardiographic nomenclature and conventions: revised and extended. Circulation 1956;14:435-50.

Skolnik, M.I. (1990), *Radar Handbook*, 2nd Ed., R-SCGraw-Hill, New York, 1990.

Staderini, E.M. (2002a). UWB radars in medicine. *Aerospace and Electronic Systems Magazine, IEEE*, Vol. 17, No.1, pp. 13-18, Jan 2002.

Starr, I.; Noordergraaf, A. (1967) *Ballistocardiography in Cardiovascular Research*. Philadelphia: Lippincott, 1967.

Staderini, E.M. (2002b). An UWB radar based stealthy 'lie detector'. *Second Virtual Congress of HRV Scientific Material,* 2002.

Such, O., et al. (2006). On-body sensors for personal healthcare, in B. Spekowius and T. Wendler editors, *Advances in Health Care Technology: Shaping the Future of Medical Care*, Vol. 6, pp. 436–488, Springer, 2006.

Tavakolian, K.; Zadeh, F.M.; Chuo, Y.; Vaseghi, A. & Kaminska, B. (2008a). Development of a Novel Contactless Mechanocardiograph Device. *Int. J. Telemedicine Appl.,* 2008:436870.

Tavakolian, K.; Vaseghi, A.; Kaminska, B. (2008b). "Improvement of ballistocardiogram processing by inclusion of respiration information" *Journal of Physiological Measurement*, Institute of Physics, 29 (2008) 771-781.

Thansandote, A.; Stuchly, S.S.; Smith A.M. (1983). Monitoring variations of biological impedances using microwave Doppler radar. *Physics in Medicine & Biology*, 1983.

Thijs, J.A.J.; Muehlsteff, J.; Such, O.; Pinter, R.; Elfring, R. & Igney, C.H. (2005). A Comparison of Continuous Wave Doppler Radar to Impedance Cardiography for Analysis of Mechanical Heart Activity, *Engineering in Medicine and Biology Society (IEEE-EMBS), 27th Annual Int. Conf.*, Sep. 2005.

Biomedical Engineering

Edited by Carlos Alexandre Barros de Mello

Biomedical Engineering can be seen as a mix of Medicine, Engineering and Science. In fact, this is a natural connection, as the most complicated engineering masterpiece is the human body. And it is exactly to help our "body machine" that Biomedical Engineering has its niche. This book brings the state-of-the-art of some of the most important current research related to Biomedical Engineering. I am very honored to be editing such a valuable book, which has contributions of a selected group of researchers describing the best of their work. Through its 36 chapters, the reader will have access to works related to ECG, image processing, sensors, artificial intelligence, and several other exciting fields.

How to reference

In order to correctly reference this scholarly work, feel free to copy and paste the following:

INTECH
open science | open minds